Journal of Thermal Science Vol.27, No.2 (2018) 184–194

https://doi.org/10.1007/s11630-018-0999-y **Article ID: 1003-2169(2018)02-0184-11**

Comparative Study of Convective Heat Transfer Performance of Steam and Air Flow in Rib Roughened Channels

MA Chao[1], JI Yongbin[2], GE Bing[2], ZANG Shusheng[2], CHEN Hua[1]

1. Marine engineering college, Dalian Maritime University, Dalian 116026, China
2. School of Mechanical Engineering, Shanghai Jiao Tong University, Shanghai 200240, China

A comparative experimental study of heat transfer characteristics of steam and air flow in rectangular channels roughened with parallel ribs was conducted by using an infrared camera. Effects of Reynolds numbers and rib angles on the steam and air convective heat transfer have been obtained and compared with each other for the Reynolds number from about 4,000 to 15,000. For all the ribbed channels the rib pitch to height ratio (p/e) is 10, and the rib height to the channel hydraulic diameter ratio is 0.078, while the rib angles are varied from 90° to 45°. Based on experimental results, it can be found that, even though the heat transfer distributions of steam and air flow in the ribbed channels are similar to each other, the steam flow can obtain higher convective heat transfer enhancement capability, and the heat transfer enhancement of both the steam and air becomes greater with the rib angle deceasing from 90° to 45°. At Reynolds number of about 12,000, the area-averaged Nusselt numbers of the steam flow is about 13.9%, 14.2%, 19.9% and 23.9% higher than those of the air flow for the rib angles of 90°, 75°, 60° and 45° respectively. With the experimental results the correlations for Nusselt number in terms of Reynolds number and rib angle for the steam and air flow in the ribbed channels were developed respectively.

Keywords: steam cooling, air cooling, rib-roughened channel, gas turbine, heat transfer

Introduction

Efficiency and power output of gas turbine can be improved significantly through increasing turbine inlet temperature. In order to keep turbine vanes and blades from thermal damage, many cooling techniques have been applied in modern turbines including film cooling, transpiration cooling, impingement cooling and rib/pin roughened cooling techniques. Rib turbulators are often used in the mid-section ducts inside the vanes and blades to increase the forced convective heat transfer. The ribs lead to flow separation, reattachment, and strong secondary flow in the mainstream, and therefore it is very important to predict the heat transfer characteristics in ribbed ducts accurately. Rib roughened cooling attracted numerous investigations in traditional air cooling technologies.

Han et al [1] addressed effects of rib shape, angle of attack, and pitch-to-height ratio. According to these investigators, ribs with 45° inclinations produce better heat transfer performance than ribs with 90° orientations, when compared at the same friction power. Han et al [2] provided heat transfer results for square and rectangular turbulated channels with different rib spacing. Han et al [3] studied the heat transfer augmentation with a variety of rib configurations. They showed that complex rib for-

Received: October 30, 2017 MA Chao: Lecturer, PhD. E-mail: iammach@163.com
This research was funded by the National Natural Science Foundation of China (Funding No.51206109)

Nomenclature

W	channel width, mm	T_{out}	temperature of the steam at the outlet, K
H	channel height, mm	Q_{net}	heat flux provided by heat plate, J
D_h	hydraulic diameter of the channel	Q_T	total heating power, J
E	rib width or rib height, mm	U	voltage provided by DC, V
e/D_h	relative roughness height	I	current provided by DC, A
P	rib pitch, mm	Q_{loss}	heat loss dissipating to the environment, J
P/e	rib pitch-to-height ratio	Nu	Nusselt number
A	rib angle, °	Nu_{local}	local Nusselt number
V	the velocity in the channel, m/s	Nu_{ave}	area-averaged Nusselt number
Re	Reynolds number, based on hydraulic diameter of the channel	Pr	Prandtl number
h	heat flux, W/m^2	c_p	specific heat at constant pressure
A	area of the heat plate, m^2	**GREEK SYMBOLS**	
T_w	temperature on target plate, K	ρ	density, kg/m^3
T_s	temperature of the steam in the channel, K	μ	dynamic viscocity, kg/(m·s)
T_{in}	temperature of the steam at the inlet, K	λ	thermal conductivity, W/(m·K)

mations can enhance heat transfer without imposing significant penalty on pressure drop. Ekkad and Han [4] used a transient liquid crystal technique to determine detailed Nusselt numbers in a ribbed two-pass duct. They varied channel Reynolds numbers and rib geometries for a square duct. They clearly showed the local enhancement caused by flow separation and reattachment downstream of the ribs and the associated secondary flow induced heat transfer enhancement. In addition, some other investigations were also conducted by Han et al. [5-8]. An experimental investigation of forced convection Nusselt number in a rectangular channel (aspect ratio AR = 5) with 45° rib turbulators was conducted by Tanda [9]. Effects of the Reynolds number and rib pitch-to-height ratio on local heat transfer were studied. He found that the optimal rib pitch-to-height ratio is 13.33 for the one-ribbed wall channel and p/e = 6.66–10 is optimal for the two-ribbed wall channel. Detailed Nusselt number distributions for narrow diverging channels with and without enhancement features have been obtained by Ekkad et al [10], the cooling configurations considered include rib turbulators and dimples on the heat transfer surfaces, they found that dimpled surfaces provide appreciably high Nusselt numbers and reasonable pressure drop whereas ribbed ducts provide significantly higher Nusselt numbers and higher overall pressure drop. Heat transfer coefficients and friction factors in a 45 deg V-shaped rib roughened square duct at high Reynolds numbers were measured by Alkhamis et al [11]. Reynolds numbers in their study range from 30,000 to 400,000. Results showed that 45 deg V-shaped ribs acquired a higher thermal performance than corresponding 45 deg angled ribs. The friction factor is found to be independent of the Reynolds number. Rallabandi et al. studied the effect of rib spacing (P/e) and blockage ratio (e/D) on heat transfer coefficients and friction factors with 45 deg sharp angled [12] and round angled [13] ribs in a square channel at high Reynolds numbers (up to 400,000). Correlations developed in earlier literature for lower Reynolds numbers were extended to higher Reynolds numbers.

Over the past several decades, most gas turbines have utilized air extracted from turbine compressors as a coolant. However, as the gas temperature increasing, traditional air cooling technologies become hardly to meet the requirement. Steam, with greater heat capacity than air, has been used as a new coolant in internal cooling channels in turbine vanes to improve cooling efficiency. Using steam as the coolant could reduce the air pumped from the compressor in gas turbine and then improve the efficiency of the gas turbine system. Therefore, steam cooling draws many attentions. Several manufacturers of gas turbines have significantly increased their efforts on developing machines for commercial operation. In particular, GE power systems have developed its so-called "H technology" in recent years. The basic strategy of the technological approach has been presented by Cormon [14, 15]. Bohn et al [16] presented detailed experimental and numerical investigations of the thermal load of a steam-cooled vane. Their measurements can be used to create a data base for steam-cooled vanes, which can also serve for the validation of numerical codes. Liu et al [17] did an experimental study on heat transfer coefficient in steam-cooled rectangular channel and developed the semi-empirical correlations for his test channels. Wang et al [18] numerically investigated the flow and heat transfer characteristics of steam in two-pass square channels with 45° ribbed walls under stationary and rotating con-

ditions. They found that complex secondary flow pattern leads to strong anisotropic turbulence and high level of anisotropy of Reynolds stresses, which have a significant impact on the local Nusselt number distributions. Shui et al [19, 20] compared the heat transfer between steam and air flow in a square duct. They found that the Nusselt number of steam is about 12-25% higher than that of air under the same operating condition. In addition, a steam/mist cooling technology was investigated by Li et al [21], Wang et al [22] and Guo et al [23-25], they found that mist/steam cooling technology could improve heat transfer greatly.

In this paper, IR camera was used to investigate the distributions of the forced convection Nusselt number in a rectangular channel cooled by superheated steam and air. Parallel ribs were set into the channel, and the influence of Reynolds number (Re=3070-14800 for steam and 4240-14630 for air), and rib angle (a=90°, 75°, 60°, 45°) on heat transfer of rib roughened channels were investigated. To explore the superiority of heat transfer for steam cooling to air cooling in rib-roughened channels, the local and area-averaged Nusselt numbers for the two coolants are compared with each other. Finally, based on experimental results in the paper, empirical correlations for steam cooling and air cooling were regressed, which are convenient for designing rib-roughened cooling construction in turbine vanes/blades for the above two cooling system respectively.

Experimental setup

Figure 1 shows a schematic diagram of the test rig. The main components of the rig are a test section, gas heater, steam supply system, air supply system and measuring equipment. The steam coolant is produced by a steam generator, which is heated by a gas heater (0~3kW) to 120℃ and maintained in superheated state. The air is given by an air compressor and also heated by the previously mentioned gas heater. The estimated parameters of the steam and air in the experiments are listed in Table 1 and Table 2, respectively. The top wall of the rectangular channel, made of constantan foil which also acts as a heater wall, is firmly clamped by cooper electrodes. The constantan foil is only 0.02mm thickness and its back side is covered with a layer of black heat-resistant paint which is about 0.01mm thickness, so the temperature measured on the back side of the foil is considered to be the same as that on the cooling side. The constantan foil, heated by an adjustable power supplied by DC whose output voltage and current are 0~6V and 0~200A, respectively, which could provide a constant heat flux boundary. A piece of quartz glass, could make approximate 90% infrared ray through it, is covered on the back of the constantan foil to protect it. The outside of all the metallic pipes and the test section was wrapped by multi- layers of asbestos tape to keep the system in adiabatic state.

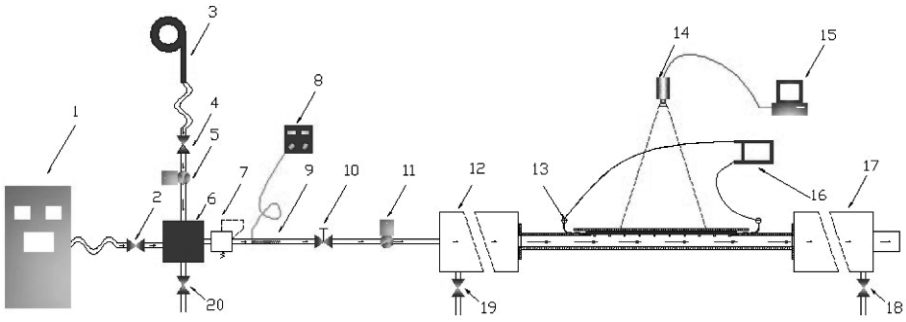

1. Steam generator 2,4,18,19,20. Ball valve 3. Air compressor 5. Air flow meter 6, 12, 17.Plenum chamber 7. Pressure maintaining valve 8. Voltage regulator 9. Gas heater 10.Regulating valve 11. Steam flow meter 13. Electrode 14. Infrared thermal camera 15. Computer 16. Direct current (DC) power supply

Fig. 1 Schematic diagram of the experimental system

Table1 Air properties

Parameter	Unit	Value
P	MPa	0.1
T	℃	35
ρ	kg/m^3	1.146
μ	kg/(m·s)	16.5E-6
λ	W/(m·℃)	0.0272
c_p	kJ/(kg·℃)	1.005
Pr	-	0.700

Table 2 Superheated steam properties

Parameter	Unit	Value
P	MPa	0.1
T	℃	120
ρ	kg/m^3	0.558
μ	kg/(m·s)	13.02E-6
λ	W/(m·℃)	0.0265
c_p	kJ/(kg·℃)	2.019
Pr	-	0.992

For steam cooling experiment, ball valve 4 in Figure 1 should be kept in closed state, the steam flows through ball valve 2, pressure maintaining valve 7, gas heater 9, steam flow meter and then flows into test section to cool the heated foil. When ball valve 2 is closed and ball valve 4 is open, the air cooling experiment starts.

The distributions of the temperature on the rib roughened foil cooled by steam and air are both measured by a VarioTHERM II infrared (IR) camera which is positioned on the back side of the foil assembly vertical to it. Every thermal image measured by the IR camera should be corrected by a correction formula which could calibrate the temperature measured by IR camera. Two thermocouples were installed in the inlet and outlet of the test section respectively to measure temperatures of the two places. Temperatures obtained by IR camera and thermocouples have uncertainties of ±0.1K and ±0.5K, respectively. The flow rate of air is measured by air flow meter with an accuracy of ±1.5%, and that of steam is obtained by a steam flow meter which has an accuracy of ±2.0%. The required mass flow rates of air and steam corresponding to Re are both controlled by a regulated valve.

Rib configurations

The typical geometry of the rib-roughened wall is shown in Fig. 2. All configurations of rib-roughened walls have a rib height-to-hydraulic diameter ratio (e/D_h) of 0.078, the rib pitch-to-height ratio (P/e) is 10 and the ribbed channel width-to-height (W/H) is fixed at 3. Four rib angles (α) have been identified for investigations. An overview of parameters for all the test cases is given in Table 3.

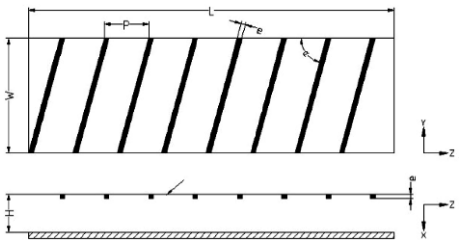

Fig. 2 Geometry of the ribbed heated surface

Table 3 The configuration parameters of the 4 test channels

Channel	e/D_h	W/H	P/e	α (°)
I	0.078	3	10	90
II	0.078	3	10	75
III	0.078	3	10	60
IV	0.078	3	10	45

Data reduction and Uncertainty analysis

Data reduction

Following equations have been used for the determinations of Reynolds number 'Re' and Nusselt number 'Nu':

The Re based on the hydraulic diameter of channel is defined as:

$$\mathrm{Re} = \frac{\rho \cdot V \cdot D_h}{\mu} \tag{1}$$

The local Nusselt number is calculated based on the equation below:

$$Nu = \frac{h \cdot D_h}{\lambda} = \frac{Q_{net} \cdot D_h}{A(T_w - T_s) \cdot \lambda} \tag{2}$$

Here, $T_s = \frac{T_{in} + T_{out}}{2}$, which is calculated by an average of the temperatures of inlet and outlet.

$$Q_{net} = Q_T - Q_{loss} = UI - Q_{loss} \tag{3}$$

Where Q_{loss} is the heat loss dissipating to environment. The Q_{loss} can be obtained by conducting auxiliary experiment, which amount to 5%~21% of the Q_T. The method of the auxiliary experiment for Q_{loss} is similar to [26].

The area averaged Nusselt number is defined as follows:

$$Nu_{ave} = \frac{\int_A Nu_{local}}{A} \tag{4}$$

Uncertainty analysis

The experimental uncertainties have been determined by a standard error analysis. In the experiment, the maximum measurement error of the flow rate is ±2.0%. And that for the temperature of the coolant and the target plate are ±0.5K and ±0.1K, respectively. According to the standard error analysis method suggested by Kline and McClintock [27], the errors of Re and Nu in the experimental results are, respectively, ±2.0% and ±3.4%. In addition, errors of voltage and current supplied by DC are only ±0.01V and ±0.001A, respectively, which have a minor contribution to the uncertainty of Nu.

Results and discussion

Heat transfer characteristics

The distributions of Nusselt number for steam cooling and air cooling on rib-roughened surface with various rib angles, associated with those on smooth surface, at Re= 12000 are respectively presented in Figure 3. All the ribs, produced by heat resisting silicone which owns extreme low thermal conductivity, were glued in the pre-designed position on investigated surface by heat resistant glue. To investigate the enhancement of heat transfer on surfaces merely on account of the turbulent flow generated by the ribs, locations of the ribs on investigated surface in Fig.4 were covered with black streaks to disregard the improvement of heat transfer caused by heat conduction of rib turbulators.

If thermal picture of the entire heat transfer surface are

captured in the experiment, the IR camera needs to be adjusted to a quite high elevation from tested surface due to the small view angle of the camera (±7°). Nevertheless, according to the investigations conducted by Han[3], periodic fully developed regions of Nusselt number would be formed behind the second or third rib turbulator when air flows through a row of ribs, as a consequence, the IR camera only needs to focus on the area behind the first two ribs along the mainstream direction in our experiment for measuring heat transfer in full developed turbulence state (shown in Fig.1). For channels with rib turbulators cooled by steam and air, repeated characteristics of the distributions of heat transfer starting from the third rib are both obviously revealed in Figure 4. In contrast, a fully developed Nusselt number is taken a longer downstream distance for smooth surface.

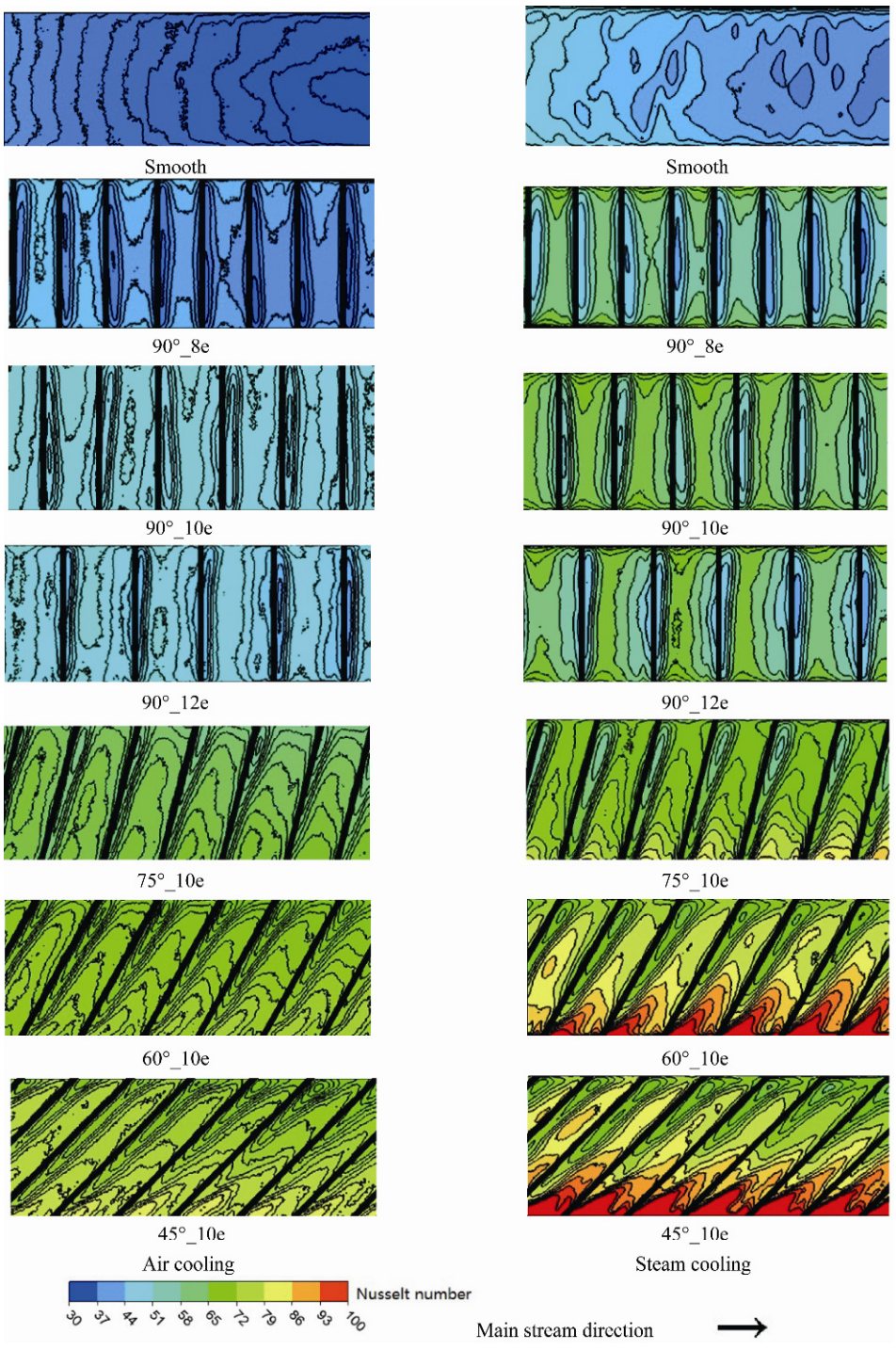

Fig. 3 Distributions of the local Nusselt number for steam cooling and air cooling on parallel rib roughened surface

In the same condition, distributions of heat transfer characteristics for steam cooling and air cooling are similar to each other, while heat transfer enhancement for steam is more intense than that for air. Based on results on 90° ribbed surface, we found that stronger heat transfer areas are developed in the middle of inter-rib regions, which ascribes to the flow reattachment in those region after the coolant flow climbs over rib turbulators. In contrast, regions with low Nusselt number near ribs (both in front of and behind ribs) can be observed obviously. Reasons for the generation of the two weak heat transfer regions are not the same: for the region in the rear of the rib, turbulent flow caused by the rib turbulator results in a low pressure area and a part of reattachment flow flows back towards this area; for the region in front of the rib, a high pressure area is generated and the separation occurs when the reattaching flow moves forward the following rib; both of the two different processes would form vortexes and flow recirculation zone occurs in front of as well as behind the rib, which serve as a reasonable explanation for the inferior mechanism of the formation of the heat transfer characteristics. Additionally, it is shown clearly that regions close to the side-walls own higher heat transfer performance, which is developed as a result of the stronger secondary flow that is generated by the interference of turbulence induced by rib turbulators and the viscous force near the walls.

From distributions of heat transfer characteristics on 75° ribbed surface, the oblique rib turbulator is found to make a conspicuous impact on the distribution of the Nusselt number. Deformation of the shape of the region with low Nusselt number behind the oblique rib is observed: compared with that of 90° rib-roughened surface, the area close to the upwind side of the rib becomes smaller. The region following the rib with low heat transfer characteristic gradually extends along the rib direction and the intensity also decreases. The region with high Nusselt number due to the reattachment of the coolant flow generates a significant expansion and a more obvious nonuniformity. The intensity of the Nusselt number in the region close to the upwind side of the rib is improved greatly and an apparent enhancement of heat transfer can be easily observed. Due to the guidance of the oblique rib, the higher temperature coolant near the bottom layer of the heat transfer surface flows along the rib, little coolant near the bottom layer could cool the surface close to the upwind rib side, and the coolant originating from middle section of the duct impinges on that area as a supplement and a secondary flow in the channel is formed to result in a stronger heat transfer performance. When the hot coolant on the bottom layer is induced to flow along the rib, it climbs over the rib to reattach the back region of the rib gradually. The phenomenon that the intensity of Nusselt number in the inter-rib region decreases gradually along the rib is understandable when considering the relative higher temperature of the fluid on the bottom layer near the heat exchange surface. Another difference from 90° ribbed surface is that distributions of low Nusselt number in front of the rib almost disappear. However, a small area with extremely high intensity of heat transfer is developed in front of the upwind side of the rib, which mainly attributes to the intense secondary flow evoked by the sudden deflection of the coolant generated by the oblique rib. Additionally, the two regions with high Nusselt number formed by the interference of the turbulence induced by ribs and the viscous force near the channel side-walls mentioned before almost disappear when the oblique angle of the parallel ribs changes from 90° to 75°.

With the rib angle decreasing, greater heat transfer enhancement is obtained on heat transfer surface. It could be explained that more coolant near the heat transfer surface will be guided along the rib direction in smaller angle ribbed channel, the secondary flow in the channel will also be aggravated. It is also found that though difference exists between 60° and 45° rib-roughened surface in the distribution of the heat transfer characteristics, the intensities of both the highest and lowest Nusselt number between the two oblique angle surface indicate no obvious distinctions and both of them are apparently higher than that of 75°. To sum up, the secondary flow developed by guiding effect of the oblique ribs mixes with the mainstream, which would result in an obvious enhancement of the heat transfer on the ribbed surface compared with that of 90° transverse ribbed surface.

Comparisons between local Nusselt number for steam cooling and air cooling along the centerline of rib roughened surface with different rib angles are respectively plotted in Figure 4. Peaks and troughs of local Nusselt number for the two coolants are almost in the same position along ‘Z’ direction. Troughs of local Nusselt number for 90° ribbed channel appear in the place about 1e away from rib turbulators and peaks of that due to flow reattachment are formed in the middle of inter-rib region. With rib angle decreasing, the secondary flow induced by oblique ribs is more intense, then thermal boundary layer near heat transfer surface is damaged more seriously, which leads to the change of the distribution of local heat transfer for different angle ribbed surface. As shown in Figure 4, peaks of local Nusselt number are closer to the following rib turbulators for the smaller ribbed surface, while troughs of that seems to change little. Nusselt number of steam cooling is higher than that of air cooling along the centerline on the heat transfer surface, especially in peak value region. In contrast, deviations of the Nusselt number between the two coolants are extremly small in flow recirculation zone in rear of rib turbulators, however, the deviation varies with different rib angle. For

90° ribbed channel, troughs of Nusselt number for steam cooling obtain higher value than that for air cooling. Troughs of Nusselt number for the two coolant are almost the same for the channel with 75° rib turbulator. As the rib angle reducing further, troughs of Nusselt number for air cooling surpass that for steam cooling.

Area-averaged heat transfer

The area-averaged Nusselt number for steam cooling and air cooling in rib-roughened channel with various rib angles are plotted in Figure 4. The Nusselt number increases with reducing Reynolds number for both the two coolants and tendencies of Nusselt number vs. Reynolds number for them are also similar to each other. Heat transfer coefficients on oblique ribbed channels are obviously higher than that on 90° ribbed one and the area-averaged Nusselt number increases with decreasing rib angle. The strongest heat transfer enhancement is obtained in 45° ribbed channel for both steam cooling and air cooling. Comparing the heat transfer coefficients be-

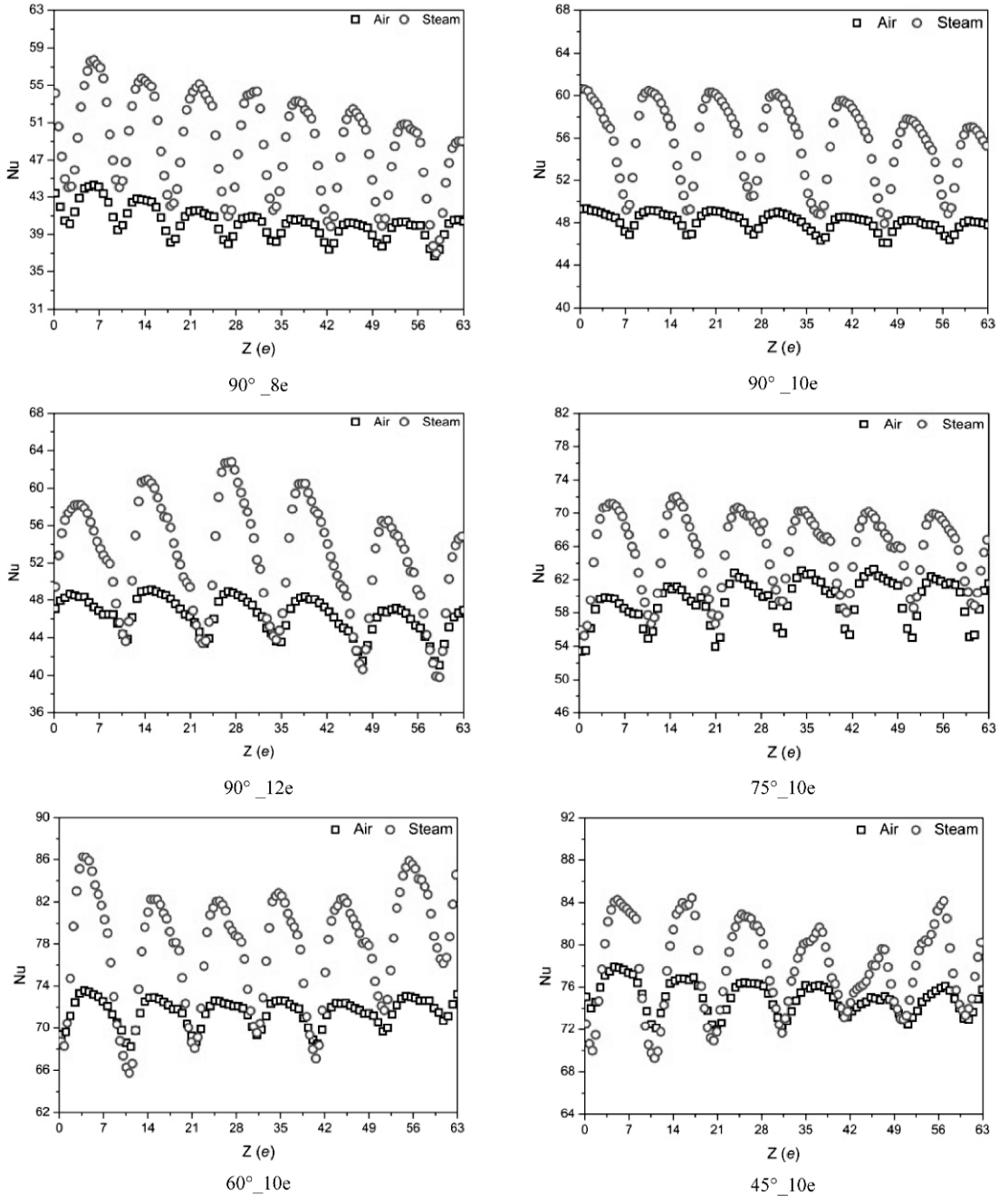

Fig. 4 Local Nusselt number along the centerline of the rib- roughened surface with different rib angle

tween the two coolants, it is found that steam has greater heat transfer performance than air in all the ribbed channels. For example, in Re=12,000 condition, area-averaged Nusselt number of steam cooling is about 13.9%, 14.2%, 19.9% and 23.9% higher than that of air cooling in 90°, 75°, 60° and 45° ribbed channel, respectively.

In order to verify the accuracy of the experimental data, area-averaged Nusselt numbers of fully developed region on smooth surface cooled by air and steam are also compared with those acquired from the Dittus-Boelter correlation, which is shown below:

$$Nu = 0.023\,\mathrm{Re}^{0.8}\,\mathrm{Pr}^{0.4} \tag{5}$$

Where Pr=0.7 and 0.99 are respectively for air and steam flow.

Based on comparison results shown in Figure 6, it is found that the averaged deviations of experimental values of the Nusselt number for air and steam flow are 4.3% and 4.7% respectively from values predicted by Equation (5).

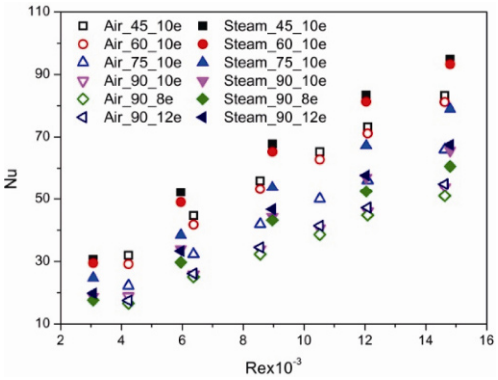

Fig. 5 Comparison of area-averaged Nusselt number for steam cooling and air cooling in ribbed channel with various rib angles

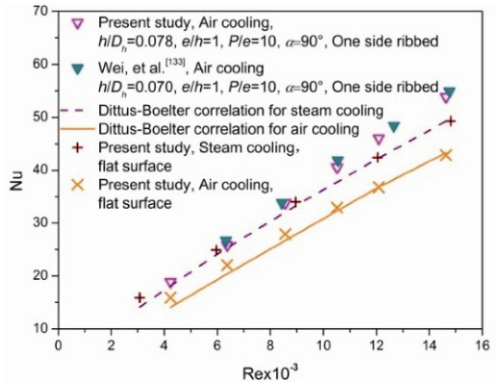

Fig. 6 Verification of the experimental results

Besides, Wei, et al[28] also have conducted an experiment to measure Nusselt number by IR camera and thermocouples on a 90° parallel ribbed channel cooled by air flow, whose geometry is quite similar to one type ribbed channel in present study. The two experimental results are compared with each other and shown in Figure 6. It is found that Nusselt numbers obtained by the present study for air cooling are all very close to those obtained by Wei, et al., which could be regarded as a further verification.

Thus, based on the above verification, it is concluded that the data for Nusselt number acquired from the present experimental setup is reliable.

Correlations for Nusselt number

It is seen that area-averaged Nusselt number for steam cooling and air cooling are both strong functions of flow parameter (Re) and rib angle (α). For the experimental section (AR=3, D_h=0.078), the function relationships for Nusselt number of steam cooling and air cooling can therefore be written as:

$$\text{Air:}\quad Nu_A = f_1(\mathrm{Re}, \alpha) \tag{6}$$

$$\text{Steam:}\quad Nu_S = f_2(\mathrm{Re}, \alpha) \tag{7}$$

To simplify the value of rib angle (α), the functions can be obtained as follows:

$$\text{Air:}\quad Nu_A = f_1(\mathrm{Re}, \alpha/60°) \tag{8}$$

$$\text{Steam:}\quad Nu_S = f_2(\mathrm{Re}, \alpha/60°) \tag{9}$$

Corresponding to correlations presented in [29-31], we can find that function of Nusselt number vs. Re and rib angle (α) is in the following form:

$$Nu_X = a \times \mathrm{Re}^b \times (\alpha/60°)^c \ (\mathrm{X=A\ or\ S}) \tag{10}$$

Figures 7 and 8 depict the experimental data represented by Nusselt number vs. Reynolds numbers for air cooling and steam cooling, respectively. Regression analyses for the two coolants yield that:

$$\text{Air:}\quad Nu_A = d_1\,\mathrm{Re}^{0.838} \tag{11}$$

$$\text{Steam:}\quad Nu_S = d_2\,\mathrm{Re}^{0.743} \tag{12}$$

Where d_1 and d_2 are not constants, they are both function of rib angle (α). Now taking '$\alpha/60°$' as a parameter into consideration, the functions can be formed as:

$$\text{Air:}\quad Nu_A/\mathrm{Re}^{0.838} = d_1 = e_1(\alpha/60°)^{c_1} \tag{13}$$

$$\text{Steam:}\quad Nu_S/\mathrm{Re}^{0.743} = d_2 = e_2(\alpha/60°)^{c_2} \tag{14}$$

Based on experimental data, fitting lines of function (13) and (14) are respectively shown in Figure 9 and 10. From regression analyses, we obtain that e_1=0.0244; c_1=-0.734; d_2=0.0696; e_2=-0.600. Correlations for Nusselt number for steam cooling and air cooling are respectively developed in the following forms:

$$\text{Air:}\quad Nu_A = 0.0244\,\mathrm{Re}^{0.838}(\alpha/60°)^{-0.734}$$
$$(4{,}240 \le \mathrm{Re} \le 14{,}630,\ 45° \le \alpha \le 90°) \tag{15}$$

$$\text{Steam:}\quad Nu_S = 0.0696\,\mathrm{Re}^{0.743}(\alpha/60°)^{-0.600}$$
$$(3{,}070 \le \mathrm{Re} \le 14{,}800,\ 45° \le \alpha \le 90°) \tag{16}$$

Where, ranges of application for the two correlations have also been provided.

Figures 11 and 12 show the comparison of Nusselt number between experimental data and values predicted by respective correlations (15) and (16). It can be seen that most of data points for the two coolants lie within the deviation lines of $\pm 10\%$. So, correlations developed in the paper for Nusselt number of steam cooling and air cooling are both reliable.

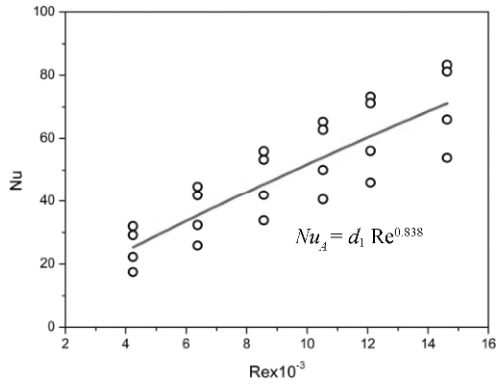

Fig. 7 Plot of Nusselt number vs. Reynolds number for air cooling

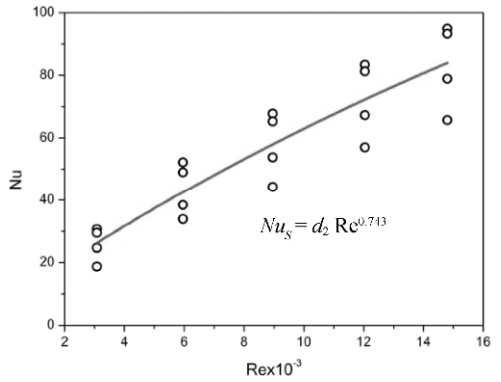

Fig. 8 Plot of Nusselt number vs. Reynolds number for steam cooling

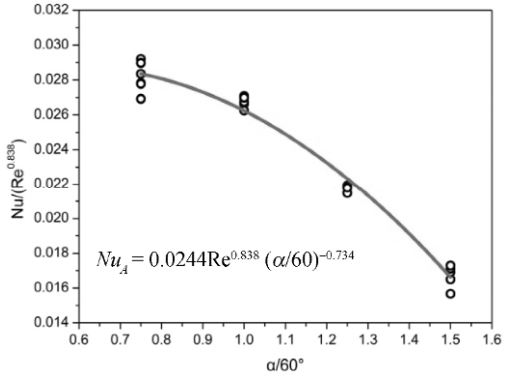

Fig. 9 Plot of $\mathrm{Nu/Re}^{0.838}$ vs. $\alpha/60°$ for air cooling

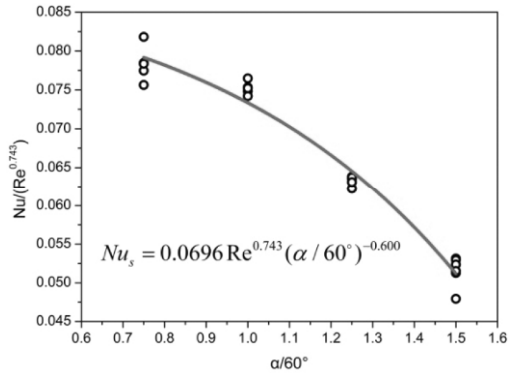

Fig. 10 Plot of $\mathrm{Nu/Re}^{0.743}$ vs. $\alpha/60°$ for steam cooling

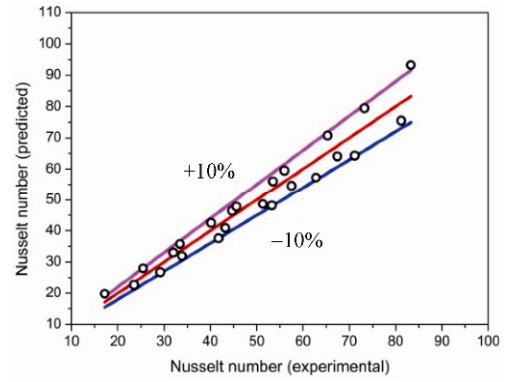

Fig. 11 Nusselt number (predicted by correlation of air cooling) vs. Nusselt number (experimental)

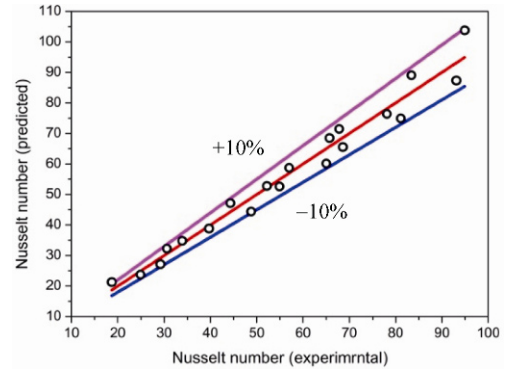

Fig. 12 Nusselt number (predicted by correlation of steam cooling) vs. Nusselt number (experimental)

Conclusions

The heat transfer characteristics of the steam and air flow in rib-roughened channel with various rib angles (a=90°,75°,60°and 45°) were experimentally investigated in the present study. Nusselt number distributions have been obtained on the endwall surface of the ribbed channels by using an infrared (IR) camera. The main conclusions of the present study can be drawn as follows:

1. The heat transfer distribution of the steam and air

flow in the ribbed channel are quite similar to each other. For the 90° ribbed channel, the area with lower heat transfer is located both before and behind the rib turbulators, and the area with higher heat transfer mostly exists in the middle region between the ribs. Angled rib turbulators have obvious positive effects on the heat transfer enhancements for both the steam and air flow. Greater heat transfer enhancement is obtained in the region close to the upwind side of rib turbulators, however the Nusselt number values decreases along the rib pointing direction.

2 Rib angles have significant influences on the Nusselt number distribution, which also distinctively affect the area-averaged heat transfer. The averaged Nusselt numbers for the steam and air both increase with the rib angle decreasing from 90° to 45°. The greatest heat transfer coefficients for the two coolants are both obtained in the 45° ribbed channel in the present investigations.

3. The steam has superior heat transfer performance to the air under the same flow condition. At Re=12,000 condition, the area-averaged Nusselt numbers of the steam flow are about 13.9%, 14.2%, 19.9% and 23.9% higher than those of the air flow in the 90°, 75°, 60° and 45° ribbed channels respectively.

4. Correlations for the Nusselt numbers are respectively developed for the steam and air flow in rib-roughened channels, which can be useful for the design of gas turbine cooling.

Acknowledgement

This research was funded by the National Natural Science Foundation of China (Funding No.51206109)

References

[1] J.C. Han, L.R. Glicksman, W.M. Rohsenow, An investigation of heat transfer and friction for rib-roughened surfaces, Int. J. Heat Mass Transfer 21 (7) (1978) 1143–1156.

[2] Han, J.C., 1988, “Heat Transfer and Friction Characteristics in Rectangular Channels with Rib Turbulators,” ASME Journal of Heat Transfer, Vol. 110, May, pp. 321–328.

[3] Han, J.C., Zhang, Y.M., Lee, C.P., 1991, “Augmented Heat Transfer in Square Channels with Parallel, Crossed, and V-Shaped Ribs,” ASME Journal of Heat Transfer, Vol.113, Oct., pp. 590–596.

[4] Ekkad, S.V., and Han, J.C., 1997, “Detailed Heat Transfer Distributions in Two-Pass Square Channels with Rib Turbulators,” International Journal of Heat and Mass Transfer, Vol. 40, No.11, pp. 2525–2537.

[5] J.C. Han, Heat Transfer and Friction in Channels With Two Opposite Rib-Roughened Walls, ASME Journal of Heat Transfer, vol.106, pp.774–781, 1984.

[6] J.C. Han, J.S. Park and C.K. Lei, Heat Transfer Enhancement in Channels with Turbulence Promoters, ASME Journal of Eng. for Gas Turbines and Power, vol.107, pp.628–635, 1985.

[7] J.C. Han, S. Ou, J.S. Park and C.K. Lei, Augmented Heat Transfer in Rectangular Channels of Narrow Aspect Ratios With Rib Turbulators, Int. J. Heat Mass Transfer, vol.32, pp.1619–1630, 1989.

[8] J.C. Han, Y.M. Zhang and C.P. Lee, Augmented Heat Transfer in Square Channels With Parallel, Crossed, and V-Shaped Angled Ribs, ASME Journal of Heat Transfer, vol.113, pp.590–596, 1991.

[9] G. Tanda. Effect of rib spacing on heat transfer and friction in a rectangular channel with 45° angled rib turbulators on one/two walls. International Journal of Heat and Mass Transfer 54 (2011) 1081–1090.

[10] J. Lamont, S. Ramesh, and S. Ekkad et al. Heat transfer enhancement in narrow diverging channels, Proceedings of ASME Turbo Expo 2012, June 11-15, 2012, Copenhagen, Denmark, GT2012-68486.

[11] N. Y. Alkhamis, A. P. Rallabandi and J. C. Han. Heat Transfer and Pressure Drop Correlations for Square Channels With V-Shaped Ribs at High Reynolds Numbers. ASME Journal of Heat Transfer, November 2011, Vol. 133 / 111901-1.

[12] Rallabandi, A. P., Yang, H., and Han, J.C., 2009, “Heat Transfer and Pressure Drop Correlations for Square Channels With 45 Deg Ribs at High Reynolds Numbers,” ASME J. Heat Transfer, 131(7), pp. 071703.

[13] Rallabandi, A. P., Alkhamis, N. Y., and Han, J. C., 2011, “Heat Transfer and Pressure Drop Measurements for a Square Channel With 45 Deg Round Edge Ribs at High Reynolds Numbers,” ASME J. Turbomach., 133(3), p. 031019.

[14] Corman J.C. H gas turbine combined cycle power generation system for the future, in Proceedings of the Yokohama Gas Turbine Congress, 1995. IGTC-paper-143, Yokohama, Japan.

[15] Corman, J. (1996), " 'H' Gas Turbine Cycle Technology & Development Status", ASME-paper 96-GT-11.

[16] D. Bohn, A. Wolff, M. Wolff et al. Experimental and numerical investigation of a steam-cooled vane. Proceedings of ASME Turbo Expo 2002. June 3-6, 2002, Amsterdam, The Netherlands. GT2002-30210.

[17] Liu J.Z., Gao J.M., Gao T.Y. Heat transfer characteristics in steam cooled rectangular channels with two opposite rib-roughened walls. Applied Thermal Engineering, Vol. 50(2013): 104–111.

[18] Wang W., Gao J.M. Flow and Heat Transfer Characteristics in Rotating Two-pass Channels Cooled by Super-

heated Steam, Chinese Journal of Aeronautics 25 (2012) 524–532.

[19] Shui L.Q., Gao J.M., Shi X.J. Effects of duct aspect ratio on heat transfer and friction in steam-cooled ducts with 60-angled rib turbulators. Experimental Thermal and Fluid Science 49 (2013) 123–134.

[20] Shui L.Q., Gao J.M., Xu L., Wang X.J. Numerical investigation of heat transfer and flow characteristics in a steam-cooled square ribbed duct, in: proceedings of ASME Turbo Expo 2010, Glasgow, UK, 2010, GT 2010 -22407.

[21] Li X., Gaddis J.L., Wang T.. Mist/steam cooling by a row of impinging jets. International Journal of Heat and Mass Transfer 46 (2003) 2279–2290.

[22] Wang T., Gaddis J.L. and Li X.C. Mist/steam heat transfer of multiple rows of impinging jets. International Journal of Heat and Mass Transfer 48 (2005) 5179–5191.

[23] Guo T., Wang T., Gaddis J.L. Mist/steam cooling in a heated horizontal tube, Part 1: Experimental system, ASME J. Turbomach. 122 (2000) 360–365.

[24] Guo T., Wang T., Gaddis J.L., Mist/steam cooling in a heated horizontal tube, Part 2: Results and modeling, ASME J. Turbomach. 122 (2000) 366–374.

[25] Guo T., Wang T., Gaddis J.L. Mist/steam cooling in a 180-degree tube, ASME J. Heat Transfer 122 (2000) 749–756.

[26] Y. Rao, C. Y. Wan, S. S. Zang. An experimental study of transitional flow friction and heat transfer performance of a channel with staggered arrays of mini-scale short pin fins. Proceedings of ASME Turbo Expo, Orlando, USA, GT2009-59341.

[27] Kline S.J. and McClintock F.A., Describing uncertainties in single-sample experiments, Mechanical Engineering, 1953, 75: 3–8.

[28] Wei, P., Jiang, P.X., Wang, Y.P. et al. Experimental and numerical investigation of convection heat transfer in channels with different types of ribs, Applied Thermal Engineering, 2011, 31: 2702–2708.

[29] S.V. Karmare and A.N. Tikekar. Heat transfer and friction factor correlation for artificially roughened duct with metal grit ribs. International Journal of Heat and Mass Transfer 50 (2007) 4342–4351.

[30] A. E. Momin, J.S. Saini, and S.C. Solanki. Heat transfer and friction in solar air heater duct with V-shaped rib roughness on absorber plate. International Journal of Heat and Mass Transfer 45 (2002) 3383–3396.

[31] S. Singh, S. Chander, J.S. Saini. Heat transfer and friction factor correlations of solar air heater ducts artificially roughened with discrete V-down ribs. Energy 36 (2011) 5053–5064.